Dissipative Effects on Inertial-Range Statistics at High Reynolds Numbers

Michael Sinhuber
Department of Civil and Environmental Engineering, Stanford University, Stanford, California 94305, USA

Gregory P. Bewley*
Department of Mechanical and Aerospace Engineering, Cornell University, Ithaca, New York 14853, USA

Eberhard Bodenschatz
Max Planck Institute for Dynamics and Self-Organization, 37077 Göttingen, Germany,
Institute for Nonlinear Dynamics, University of Goettingen, 37077 Göttingen, Germany,
Department of Physics, Cornell University, Ithaca, New York 14853, USA,
and Department of Mechanical and Aerospace Engineering, Cornell University, Ithaca, New York 14853, USA

(Received 7 March 2017; published 29 September 2017)

Using the unique capabilities of the Variable Density Turbulence Tunnel at the Max Planck Institute for Dynamics and Self-Organization, Göttingen, we report experimental measurements in classical grid turbulence that uncover oscillations of the velocity structure functions in the inertial range. This was made possible by measuring extremely long time series of up to 10^{10} samples of the turbulent fluctuating velocity, which corresponds to $O(10^7)$ integral length scales. The measurements were conducted in a well-controlled environment at a wide range of high Reynolds numbers from $R_\lambda = 110$ up to $R_\lambda = 1600$, using both traditional hot-wire probes as well as the nanoscale thermal anemometry probe developed at Princeton University. An implication of the observed oscillations is that dissipation influences the inertial-range statistics of turbulent flows at scales significantly larger than predicted by current models and theories.

DOI: 10.1103/PhysRevLett.119.134502

One of the distinguishing features of turbulent flows is the deviation of its statistics from Gaussian and the frequent occurrence of extreme events. Despite decades of research, an exact prediction or description of the statistics of these extreme events based upon the governing Navier-Stokes equations [1,2] is still absent. The rate at which extreme events, such as strong wind gusts in natural turbulent flows, occur are captured in the tails of the probability density function of the longitudinal velocity increment. The moments of this statistical object are the longitudinal structure functions of nth order $S_n = \langle [u(x) - u(x+r)]^n \rangle$. Here, $u(x)$ is the longitudinal velocity component aligned with the separation r, and x is the position. One of the few exact results that can be derived from the Navier-Stokes equations under the assumptions of stationarity, homogeneity, and isotropy concerns the third-order longitudinal structure function,

$$S_3(r) - 6\nu \frac{d}{dr} S_2(r) = -\frac{4}{5}\langle \epsilon \rangle r + q(r). \tag{1}$$

This relation was derived originally by Kármán and Howarth [3] for correlation functions and reformulated by Kolmogorov [4] in terms of structure functions. Here, $q(r)$ is a source term containing the information about energy injection, ν the kinematic viscosity, and $\langle \varepsilon \rangle$ the mean energy dissipation rate. In the limit of infinite Reynolds numbers, $\nu \to 0$, the second term on the left-hand side of the equation vanishes as long as the derivative remains finite. Following the classical cascade picture by Richardson [5] and the original arguments by Kolmogorov [4], there is an intermediate range of scales where neither the energy injection at the large scales nor the energy dissipation at small scales influences the statistics of the flow. In the inertial range, one obtains Kolmogorov's four-fifths law [6] predicting a power-law form for the third-order structure function:

$$S_3(r) = -\frac{4}{5}\langle \epsilon \rangle r. \tag{2}$$

The variation of the third-order structure function with the Reynolds number can be seen in Fig. 1. With the

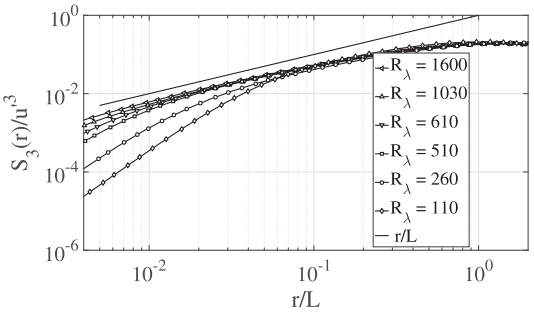

FIG. 1. Third-order structure functions measured in the Variable Density Turbulence Tunnel. Here, u' is the fluctuating velocity and L the integral length scale. The straight black line is equal to r/L, the scaling predicted by Eq. (2).

Reynolds number approaching higher values, an inertial range emerges, and the third-order structure function appears to fulfill Kolmogorov's four-fifths law.

Further assuming that the turbulent flow is self-similar [7], one can generalize the result to structure functions of arbitrary orders n, with unknown constants C_n:

$$S_n(r) = C_n(\varepsilon r)^{n/3}. \quad (3)$$

In this framework, the scaling exponents of the structure functions $\zeta_n = n/3$ are simply a linear function of the order. For real turbulent flows, the assumption of self-similarity does not hold, and numerous refined models have been proposed to describe structure functions in the inertial range [8–18]. All of these models have in common oscillation-free power-law scaling of the structure functions in the inertial range, with varying predictions for the scaling exponents as a nonlinear function of the order. Assuming the validity of these predictions, one should be able to extract scaling exponents from the data by computing logarithmic derivatives $d\log(S_n)/d\log(r) = \zeta_n$. Power-law behavior here would correspond to a horizontal line in a graph of $d\log S_n/d\log r$ against r. All deviations from this line are connected to deviations from power-law behavior (e.g., [19]). Such a graph for S_4 of our data is shown in Fig. 2. Despite the large Reynolds numbers, however, there seems to only a slow approach to true scaling.

This lack of observable scaling is a common feature in experimental turbulent flows and led to an extraction method developed by Benzi *et al.* [20] called extended self-similarity (ESS). Rather than scaling with respect to the separation r, it is proposed that structure functions scale with respect to each other, namely, $S_n \propto S_m^{\zeta_{m,n}}$ with the relative scaling exponents $\zeta_{m,n}$. Note that different definitions of S_m can influence the resulting scaling exponents

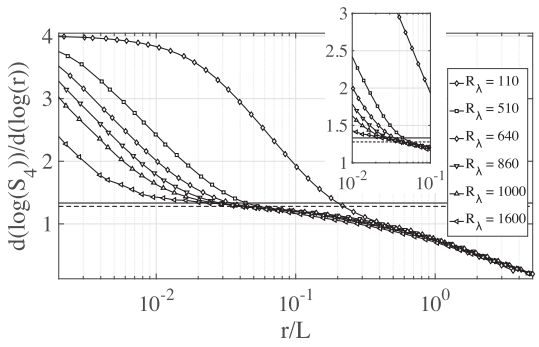

FIG. 2. Logarithmic derivative of the fourth-order structure function with respect to the separation. Even at the highest Reynolds numbers measured, there seems to be only a slow approach to a horizontal line that would correspond to power-law scaling. The solid horizontal line with $\zeta_4 = 4/3$ is the prediction by Kolmogorov [4], and the dashed line the prediction of the model by Lévêque [17]. The inset shows an enlargement of the intersection region.

[21]. We use the method to reveal the detailed shape of the structure functions.

We performed the experiments in the Variable Density Turbulence Tunnel (the VDTT) at the Max Planck Institute for Dynamics and Self-Organization [22]. The wind tunnel was a pressurizable closed-circuit wind tunnel, in which either air or sulfur hexafluoride (SF_6) circulated. By changing the pressure of the gas, we could adjust its kinematic viscosity ν, and thus the Reynolds number R_λ, without changing the geometrical boundary conditions or the mean speed of the flow. We set the pressure to values between 1 and 15 bar and so prepared viscosities between 1.55×10^{-5} and 1.42×10^{-7} m^2/s.

To produce turbulence, we used a biplanar grid of square grid bars of mesh spacing of 18 cm that blocked about 40% of the cross section l. The mean speed U of the flow was kept constant at 4.2 m/s. The temperature of the gas was stable to within 0.2 K over arbitrary times and was set to fixed values between 22.0° C and 23.4° C.

The velocity of the gas was measured at either 7.1 or 8.3 m downstream of the grid with the nanoscale thermal anemometry probe (NSTAP) developed at Princeton University [23,24]. These were microfabricated hot-wire probes, manufactured in two different ways such that they had either 30- or 60-micron-long sensor elements. In addition to the data acquired with the NSTAPs, we also acquired data with larger hot-wire probes of traditional construction produced by Dantec Dynamics, 0.45 or 1.25 mm long. The data acquired with the Dantec probes are not shown in this Letter, as these probes subject to probe size filtering effects at even moderate Reynolds numbers [22,25], but they gave results consistent with those from the NSTAP. Further details on the probe size and filtering effects can be found in Supplemental Material [26] and in the work by Hutchins *et al.* [27]. The longer data sets presented in this Letter were acquired in conjunction with those shown in our paper on the decay of turbulence [28], but the present data are much longer as needed for the different purpose of this Letter—providing sufficient statistics to uncover details of the inertial-range statistics.

The quantity measured by the hot-wire probes is the velocity time series $v(t)$ observed at a single position, low-pass filtered at either 30 or 100 kHz, and sampled at either 60 or 200 kHz, respectively. The turbulence intensity u' was between 1.6% and 3.6% of the mean speed U, which is significantly smaller than the 15% turbulence intensity that was found [29] to be sufficiently small to be able to invoke Taylor's hypothesis [30] in order to convert the functions of time, $v(t)$, to functions of space, so that $v(tU) = v(x)$ while still retaining the correct small-scale statistics and key turbulent quantities such as the energy spectrum in space. In flows with spatially [31] or temporally [32] nonstationary mean flows, the demands on the turbulence intensity are higher. However, the Variable Density Turbulence Tunnel was designed to have a well-defined

velocity profile absent of shear paired with a constant mean speed [22], so this limitation of Taylor's hypothesis is not limiting the viability of the results.

We divide the various data into two categories, which we call data sets A and B. Each data set is comprised of measurements made at different Reynolds numbers. What separates the data sets is the length of the velocity records. Data set A consisted of 14 measurements, which were each between 6 and 9 h long, or up to about 10^6 integral length scales long. Data set B consisted of four measurements, which were each between 2 and 3 days long, or up to about 10^7 integral length scales long. Take note that the amount of data obtained in these data sets exceeds any comparable experiment by an order of magnitude, making it possible to investigate fine details in the inertial-range structure of turbulence. The integral length scale for all flows was about 0.1 m. Altogether, the data sets span Taylor Reynolds numbers between 110 and 1600.

The aforementioned models considered statistics in the inertial range where, as in the classical cascade model, neither dissipation nor energy injection play a role. However, in turbulence, there is no sharp distinctive scale between the ranges where the statistics change. Even above the Kolmogorov length, dissipation influences the statistics, leading to the so-called near-dissipation range [33–35]. A model describing the effects of dissipation in the near-dissipation regime [36,37] has been developed in Meneveau [38]. He, among others [39,40], noted that an order-dependent viscous cutoff scale leads to deviations from scaling behavior in the near-dissipation range that grow larger as the Reynolds number increases. There are numerous alternative models for the near-dissipation range, for example, She [41], Biferale [42], and Chevillard, Castaing, and Lévêque [43]. Additional investigations of the transition between the dissipative and inertial ranges [44,45] detailed the bottleneck in the energy spectrum. This ringing in the energy spectrum affects the transitions between different ranges in structure functions [46–48]. We do not discriminate between the models and chose to compare our data with Meneveau's multifractal model for convenience. In the multifractal model, the structure functions are functions of both r/η and r/L:

$$S_n = f_n(r/\eta)\left(\frac{r}{L}\right)^{\zeta_n}. \tag{4}$$

Using the predictions of the p model by Meneveau and Sreenivasan [13,14], Meneveau [38] computes the functional form of $f_n(r/\eta)$. The scaling exponents of the p model are nonlinear functions of n [14]:

$$\zeta_n = 1 - \log_2\left[p^{n/3} + (1-p)^{n/3}\right]. \tag{5}$$

Allowing for an order-dependent viscous cutoff scale, Meneveau [38] shows that

$$f_n(r/\eta) = \left[1 + \left(c_a \frac{r}{\eta}(c_b R_\lambda^{3/2})^{(1-\alpha_p)/(3+\alpha_p)}\right)^{-2}\right]^{(\zeta_n - n)/2} \tag{6}$$

with abbreviations $c_a = 0.1 \times 15^{-0.75}$, $c_b = 1/13$, and

$$\alpha_p = -\frac{p^{n/3}\log_2 p + (1-p)^{n/3}\log_2(1-p)}{p^{n/3} + (1-p)^{n/3}}. \tag{7}$$

As in Meneveau [38], we set the free parameter p to 0.7. p governs how unequally energy is distributed among eddies breaking during the turbulent cascade.

Figure 3 shows ESS plots from the multifractal model. For convenience, we present the logarithmic derivative of the fourth-order structure function by the second-order structure functions using the scaling exponents given by the p model. Any other choice of structure function or scaling exponent model gives qualitatively equivalent results. The free turbulence parameters in this plot, η, L, and R_λ, are extracted from data sets A and B for five data sets between $R_\lambda = 110$ (top) and $R_\lambda = 1600$ (bottom) using Eq. (1) and the velocity autocorrelation function. In the multifractal model, there is a significant minimum in the near-dissipation range at around 20η as a result of the order-dependent cutoff scale [34]. For $r \gg 20\eta$, the logarithmic derivative approaches its expected inertial-range limit of $\zeta_{4,2}$. Within the multifractal model, there is strict power-law scaling in the structure functions as long as $r \gg 20\eta$.

It is a common procedure to extract scaling exponents from ESS plots by averaging over scales that are reasonably far away from the Kolmogorov scale, in accordance with the multifractal predictions. However, the high-Reynolds number, extremely long data sets from the VDTT demonstrate the need for a more refined interpretation. Figure 4 shows the

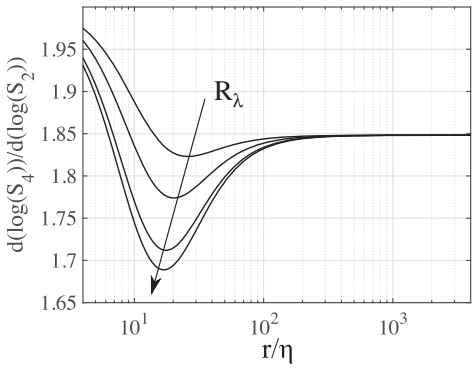

FIG. 3. Prediction for the shape of the logarithmic derivative of the fourth-order structure function with respect to the second-order structure function as given by the multifractal model [38] using the p model [13] for the scaling exponents and turbulence parameters from several VDTT data sets for R_λ between 110 and 1600. The arrow indicates the direction of increasing Reynolds number. The model predicts a single oscillation with a minimum at about 20η.

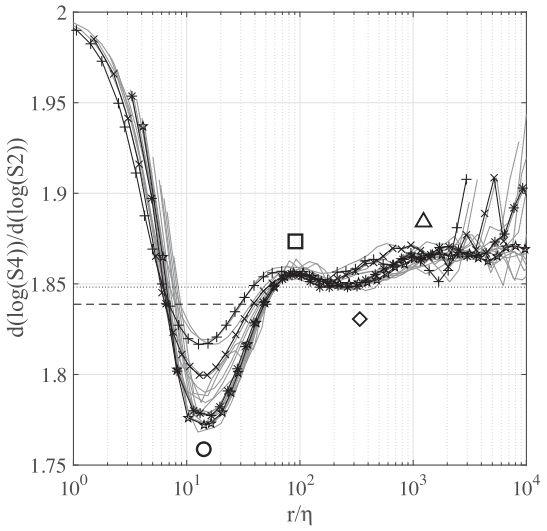

FIG. 4. Logarithmic derivative of the fourth-order structure with respect to the second-order structure function, obtained by NSTAP probes. Highlighted are four representative curves obtained with NSTAPs at $R_\lambda = 260$ (plus), $R_\lambda = 510$ (crosses), $R_\lambda = 880$ (stars), and $R_\lambda = 1030$ (pentagrams). The data span Taylor-scale Reynolds numbers from 110 to 1600. For comparison, the prediction of Lévéque [17] is indicated by a dashed line and the p model by the dotted line. Note that the prediction in Kolmogorov [6] is $d\log S_4/d\log S_2 = 2$. The near-dissipation range deviations are in agreement with the predictions of the multifractal model [38]; there is an overshoot at about 20η (circle). However, more structural details are observable in the inertial range, being uncovered by the large amount of data. These additional oscillatory features are marked by square, diamond, and triangle.

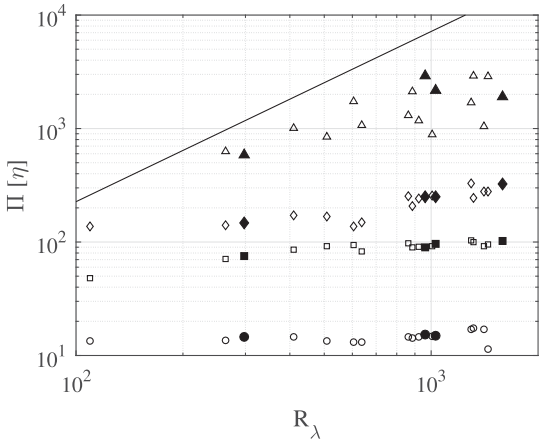

FIG. 5. The positions Π of the extrema in the logarithmic derivatives of Fig. 4 in terms of the Kolmogorov scale η and as a function of the Reynolds number R_λ. The solid black line is $0.5L/\eta$, predicted by our experiments. Circles represent the location of the near-dissipation range minimum, squares the first maximum, diamonds the second minimum, and triangles the second maximum. Open symbols correspond to data set A, solid symbols to data set B. Once the Reynolds number is high enough, the features denoted by circles, squares, diamonds, and triangles appear to be only weakly dependent on the Reynolds number.

logarithmic derivative of the fourth-order structure function with respect to the second-order structure function for the whole range of Reynolds numbers between $R_\lambda = 100$ and $R_\lambda = 1600$ in data sets A and B. In the near-dissipation range, between 10η and 30η the data are in good qualitative agreement with the predictions of the multifractal model as seen in Fig. 3. For instance, with an increasing Reynolds number, the minimum in the near-dissipation range (○) grows significantly in depth. At smaller scales, the NSTAP data are distorted by noise, and temporal and spatial filtering influences the probe response. Nonetheless, our experiments uncover features not reported in the literature. While the multifractal model predicts a monotonic approach from the near-dissipation range minimum toward the value of the ratio of the scaling exponents, the VDTT data show an overshoot (□) at around 70η, which is approximately independent of the Reynolds number. In contrast to the expectations, the data from the VDTT do not approach a constant value at higher r/η. Instead, an only weakly Reynolds-number-dependent and persistent substructure in the inertial range becomes visible.

Figure 5 shows the positions, Π, of the substructures in Fig. 4 in terms of the Kolmogorov scale and as a function of the Reynolds number. These positions have been obtained using a windowed parabolic fit to the data up to $r = 2L$, though other methods such as four-peak Gaussian fits yield comparable results. In addition to the overshoot (square) at about 70η, an additional extremum becomes apparent in Fig. 4 (diamond) before the data succumb to noise at larger r/η, potentially showing one further extremum (triangle). These structures in the inertial range become visible only with the long data sets from the VDTT at a high Reynolds number; at either lower Reynolds numbers or with significantly shorter data sets, these extrema are lost within the noise. These new inertial-range structures in the structure functions are associated with the bottleneck phenomenon in the energy spectrum in the sense that the cascade process does not uniformly transport energy across all associated scales [44], and they can be embedded in refinements of existing inertial-range models. The features are reminiscent of the lacunarity proposed by Smith, Fournier, and Spiegel [49].

These findings have significant implications for the interpretation of the statistical behavior of turbulent flows. The persistent structures in the ESS plots can be understood as a modulation of power-law behavior in the inertial range and imply an oscillatory component in the structure functions themselves, albeit small. An order-dependent cutoff scale, as in the multifractal model, is by construction unable to include multiple overshoots. A consequence is that with different choices of averaging intervals the same data yield different scaling exponents. The oscillatory behavior demands refined models of the structure

functions. The maxima and minima we find in the inertial range are not strongly dependent on the Reynolds number and are anchored to the small scales η. This unexpected behavior shows that far away from the dissipation range, far even from the near-dissipation range, dissipative effects still qualitatively affect the statistics of the flow. It is not clear from our data how far up from the dissipation range in scale the oscillations persist. Future investigations should measure at an even higher Reynolds number to achieve a higher ratio of L/η and to uncover more features of the inertial-range statistics. With an active grid installed, the VDTT is able to achieve Reynolds numbers significantly higher than the classic grid data presented here and will be such a further step.

We thank A. Renner, A. Kopp, A. Kubitzek, H. Nobach, U. Schminke, and the machinists at the Max Planck Institute for Dynamics and Self-Organization who helped to build and maintain the VDTT. The NSTAPs were developed at Princeton University by M. Vallikivi, M. Hultmark, and A. J. Smits, who graciously provided them and helped to make them work with the VDTT equipment. We are thankful to F. Köhler and L. Hillmann, who assisted in acquiring the data. We especially thank L. Biferale, C. Meneveau, K. R. Sreenivasan, W. van de Water, M. Wilczek, and V. Yakhot for fruitful discussions. The data analyzed here were taken at the Max-Planck-Institute for Dynamics and Self-Organization during the doctoral thesis work of Michael Sinhuber.

*gpb1@cornell.edu

[1] C. L. M. Navier, Mem. Acad. Sci. Inst. France **6**, 389 (1827).
[2] G. G. Stokes, Trans. Cambridge Philos. Soc. **8**, 287 (1845).
[3] T. von Kármán and L. Howarth, Proc. R. Soc. A **164**, 192 (1938).
[4] A. N. Kolmogorov, Dokl. Akad. Nauk SSSR **30**, 299 (1941).
[5] L. F. Richardson, *Weather Prediction by Numerical Process* (Cambridge University Press, Cambridge, England, 1922).
[6] A. N. Kolmogorov, Dokl. Akad. Nauk SSSR **32**, 16 (1941).
[7] S. B. Pope, *Turbulent Flows* (Cambridge University Press, Cambridge, England, 2000).
[8] L. D. Landau and E. M. Lifschitz, *Fluid Mechanics* (Pergamon, New York, 1959), translated from Russian by J. B. Sykes and W. H. Reid.
[9] A. N. Kolmogorov, J. Fluid Mech. **13**, 82 (1962).
[10] U. Frisch, P.-L. Sulem, and M. Nelkin, J. Fluid Mech. **87**, 719 (1978).
[11] R. Benzi, G. Paladin, G. Parisi, and A. Vulpiani, J. Phys. A **17**, 3521 (1984).
[12] G. Paladin and A. Vulpiani, Phys. Rev. A **35**, 1971 (1987).
[13] C. Meneveau and K. R. Sreenivasan, Nucl. Phys. B, Proc. Suppl. **2**, 49 (1987).
[14] C. Meneveau and K. R. Sreenivasan, Phys. Rev. Lett. **59**, 1424 (1987).
[15] L. C. Andrews, R. L. Phillips, B. K. Shivamoggi, J. K. Beck, and M. L. Joshi, Phys. Fluids A **1**, 999 (1989).
[16] S. Kida, J. Phys. Soc. Jpn. **60**, 5 (1991).
[17] Z.-S. She and E. Lévêque, Phys. Rev. Lett. **72**, 336 (1994).
[18] B. Dubrulle, Phys. Rev. Lett. **73**, 959 (1994).
[19] K. R. Sreenivasan and B. Dhruva, Prog. Theor. Phys. Suppl. **130**, 103 (1998).
[20] R. Benzi, S. Ciliberto, R. Tripiccione, C. Baudet, F. Massaioli, and S. Succi, Phys. Rev. E **48**, R29 (1993).
[21] W. van de Water and J. Herweijer, Phys. Rev. E **51**, 2669 (1995).
[22] E. Bodenschatz, G. P. Bewley, H. Nobach, M. Sinhuber, and H. Xu, Rev. Sci. Instrum. **85**, 093908 (2014).
[23] S. C. C. Bailey, G. J. Kunkel, M. Hultmark, M. Vallikivi, J. P. Hill, K. A. Meyer, C. Tsay, C. B. Arnold, and A. J. Smits, J. Fluid Mech. **663**, 160 (2010).
[24] M. Vallikivi, M. Hultmark, S. Bailey, and A. Smits, Exp. Fluids **51**, 1521 (2011).
[25] A. Ashok, S. C. C. Bailey, M. Hultmark, and A. J. Smits, Exp. Fluids **53**, 1713 (2012).
[26] See Supplemental Material at http://link.aps.org/supplemental/10.1103/PhysRevLett.119.134502 for a discussion of probe size and filtering effects.
[27] N. Hutchins, J. P. Monty, M. Hultmark, and A. J. Smits, Exp. Fluids **56**, 18 (2015).
[28] M. Sinhuber, E. Bodenschatz, and G. P. Bewley, Phys. Rev. Lett. **114**, 034501 (2015).
[29] S. Lee, S. K. Lele, and P. Moin, Phys. Fluids A **4**, 1521 (1992).
[30] G. I. Taylor, Proc. R. Soc. A **164**, 476 (1938).
[31] J. L. Lumley, Phys. Fluids **8**, 1056 (1965).
[32] J. F. Pinton and R. Labbé, *Advances in Turbulence V* (Kluwer Academic, Dordrecht, 1995), pp. 418–422.
[33] K. R. Sreenivasan and C. Meneveau, Phys. Rev. A **38**, 6287 (1988).
[34] U. Frisch and Vergassola, Europhys. Lett. **14**, 439 (1991).
[35] R. Benzi, L. Biferale, R. Fisher, D. Q. Lamb, and F. Toschi, J. Fluid Mech. **653**, 221 (2010).
[36] U. Frisch and G. Parisi, in *Turbulence and Predictability in Geophysical Fluid Dynamics and Climate Dynamics* (Elsevier Science, New York, 1985), Vol. 88, pp. 71–88.
[37] J. Schumacher, K. R. Sreenivasan, and V. Yakhot, New J. Phys. **9**, 89 (2007).
[38] C. Meneveau, Phys. Rev. E **54**, 3657 (1996).
[39] M. Nelkin, Phys. Rev. A **42**, 7226 (1990).
[40] R. Benzi, L. Biferale, G. Paladin, A. Vulpiani, and M. Vergassola, Phys. Rev. Lett. **67**, 2299 (1991).
[41] Z.-S. She, Phys. Rev. Lett. **66**, 600 (1991).
[42] L. Biferale, Phys. Fluids A **5**, 428 (1993).
[43] L. Chevillard, B. Castaing, and E. Lévêque, Eur. Phys. J. B **45**, 561 (2005).
[44] G. Falkovich, Phys. Fluids **6**, 1411 (1994).
[45] D. A. Donzis and K. R. Sreenivasan, J. Fluid Mech. **657**, 171 (2010).
[46] D. Lohse and A. Müller-Groeling, Phys. Rev. Lett. **74**, 1747 (1995).
[47] D. Lohse and A. Müller-Groeling, Phys. Rev. E **54**, 395 (1996).
[48] W. Dobler, N. E. L. Haugen, T. A. Yousef, and A. Brandenburg, Phys. Rev. E **68**, 026304 (2003).
[49] L. A. Smith, J.-D. Fournier, and E. A. Spiegel, Phys. Lett. **114A**, 465 (1986).